

High-Order Relation Construction and Mining for Graph Matching

Hui Xu, Liyao Xiang, Youmin Le, Xiaoying Gan, Yuting Jia, Luoyi Fu, Xinbing Wang

Shanghai Jiao Tong University

{xhui_1,xiangliyao08,leyouming,ganxiaoying,hnxxjyt,yiluofu,xwang8}@sjtu.edu.cn

Abstract

Graph matching pairs corresponding nodes across two or more graphs. The problem is difficult as it is hard to capture the structural similarity across graphs, especially on large graphs. We propose to incorporate high-order information for matching large-scale graphs. Iterated line graphs are introduced for the first time to describe such high-order information, based on which we present a new graph matching method, called High-order Graph Matching Network (HGMMN), to learn not only the local structural correspondence, but also the hyperedge relations across graphs. We theoretically prove that iterated line graphs are more expressive than graph convolution networks in terms of aligning nodes. By imposing practical constraints, HGMMN is made scalable to large-scale graphs. Experimental results on a variety of settings have shown that, HGMMN acquires more accurate matching results than the state-of-the-art, verifying our method effectively captures the structural similarity across different graphs.

Introduction

Graph matching refers to pairing corresponding nodes across two or more graphs by considering graph structural similarities and the optional attribute similarities. Since graphs are natural representations for many types of real-world data, the technique of graph matching lies at the core of many applications. Examples include but not limit to: 2D/3D shape matching for visual tracking in computer vision (Wang, Yan, and Yang 2019), user accounts linkage across different online social networks (Liu et al. 2016; Fu et al. 2020), and entity alignment in cross-lingual knowledge graphs (Wu et al. 2019; Xu et al. 2019b).

High-order information has been proven useful in graph matching theoretically and empirically (Zass and Shashua 2008; Duchenne et al. 2011). Different from the first-order (node) and second-order (edge), the high-order information is associated with specified node sets which compose connected components of a graph, typically referred to as *hyperedges*. Since corresponding nodes often share similar structures in their neighborhoods, high-order information are helpful in capturing similarity across graphs and identifying the corresponding nodes more precisely. Previous works have tried to incorporate high-order informa-

this paper is under review

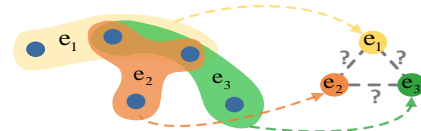


Figure 1: An illustration of hypergraphs: an edge can join any number of nodes. Previous works do not explicitly consider the relation across hyperedges.

tion for achieving better matching accuracies. Some works (Duchenne et al. 2011; Yan et al. 2015) formulate graph matching as high-order affinity tensor based model and solve it with optimization techniques. The concept of hypergraphs are introduced in the learning based framework (Tan et al. 2014) for graph matching. Recently, *Graph Convolution Networks* (GCNs) are exploited in (Wang et al. 2018; Xu et al. 2019b) to aggregate the high-order neighborhood information. It is proven that GCNs learn the hyperedges’ representations approximately.

In spite of their promising performance, prior works have not proposed a principled way to describe the high-order information on graphs. Fig. 1 gives a typical example of hypergraphs where e_1, e_2, e_3 each represents a subset of nodes on the original graph. It is worth mentioning that previous methods with high-order information merely leverage the combination of features of the corresponding nodes within one hyperedge, but ignore the relative structural information across hyperedges. However, such information plays an essential role in the characterization of social networks and molecule graphs (Morris et al. 2019).

We aim to introduce the high-order information to solve the large-scale graph matching problem by addressing the following challenges. *First*, since hypergraphs are not natural graph representations, there is no principled ways to extract hyperedges on graphs without additional node attributes, and to express the relation between hyperedges afterwards. *Second*, it is not clear how to build the relation between the similarity in hypergraphs and the similarity in the original graphs in a learning based framework. *Third*, from an engineering perspective, the consideration of the relation across hyperedges naturally introduces great complexity into the graph matching problem, and thus would be problematic to scale to large-size graphs.

To solve the first problem, we propose a learning-based graph matching method called *High-order Graph Match-*

ing Networks (HGMM), taking advantage of the high-order structural information on graphs. We novelly use *line graphs*, in particular, *iterated line graphs* (ILG) (Harary and Norman 1960), to describe the high-order structural information of a graph. Each node of the ILG can be viewed as a hyperedge of the original graph, and ILG requires no additional node attribute in its construction. Since the ILG is iteratively built from the original graph, hierarchical structural information can be described. By further taking into account the relative structural information of the ILG, we prove that GCNs cannot be more expressive than our method in aligning corresponding nodes across graphs theoretically and empirically. To resolve the second issue, we apply a general GNN to the ILG as to the original graphs for learning the embedding of each node (corresponding to the hyperedge), and establishing the high-order relations between graphs. Finally, by imposing constraints on the maximum degree of the graph, we are able to control the computational complexity of HGMM on large-scale graphs.

Highlights of contributions are as follows:

- To resolve graph matching, we introduce iterated line graphs to describe the high-order information, which is helpful in capturing the hierarchical structure of original graphs. We prove that GCNs are no more expressive than iterated line graphs in terms of aligning corresponding nodes.
- A novel GNN-based high-order graph matching method called HGMM is proposed, which can utilize high-order structural similarity to get a more accurate matching result.
- Evaluated on a variety of real-world datasets in different settings, HGMM is shown to have superior performance than the state-of-the-art graph matching methods.

Related Works

Graph matching tries to find correspondences between two graphs and is conventionally formulated as Quadratic Assignment Problem (QAP) in (Loiola et al. 2007; Cho, Lee, and Lee 2010; Zhou and De la Torre 2015). The problem is known as NP-complete and solved with optimization techniques. Works such as (Duchenne et al. 2011; Yan et al. 2015; Nguyen, Gautier, and Hein 2015) extend QAP to high-order tensor forms by encoding affinity between two hyperedges from graphs. However, the optimization-based approaches are not scalable to large-scale graphs.

There are many learning-based methods proposed to tackle graph matching, or network alignment, for large-scale inputs: IONE (Liu et al. 2016) introduces a unified optimization framework to solve the network embedding and alignment tasks simultaneously. DeepLink (Zhou et al. 2018) samples the networks by random walk and introduces a dual learning method. CrossMNA (Chu et al. 2019) performs multi-graph alignment by using the cross-network information to refine the inter- and the intra- node embedding vectors respectively. Recently, many approaches leverage GCNs to capture the high-order information for graph matching, since GCNs is capable of aggregating m -hop neighborhood information of each node by stacking m layers of GCN.

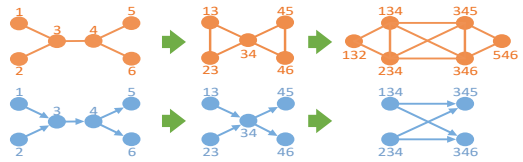


Figure 2: Construction of iterated line graphs for directed (lower) and undirected (upper) graphs.

GMNN (Xu et al. 2019b) merges the node-level and the graph-level matching results by adopting GCN layers and cross-graph attention mechanisms. DGMC (Fey et al. 2020) presents a two-stage deep neural architecture for reaching a data-driven neighborhood consensus, and proposes optimization to fit to the large input domains. Although previous works have achieved some success, GCNs-based methods do not fully take advantage of the high-order structural information. We construct iterated line graphs as powerful expressions of high-order information in this paper.

Some works explicitly propose graph matching methods using **hypergraphs**. MAH (Tan et al. 2014) is inspired by the intuition that nodes within a hyperedge should have higher similarity than the nodes belonging to different hyperedges. MGCN (Chen et al. 2020) is an enhanced version of MAH as it considers multi-level graph convolutions on both local network structures and hypergraphs in a unified way. In fact, MGCN focuses on the anchor link prediction problem, which is related to but different from the graph matching problem. Although both MAH and MGCN utilize hypergraphs, they are unable to describe graph structures of different granularities while our methods can establish hyperedges in a hierarchical way with enriched information.

Preliminaries

Hypergraphs and Hyperedges. Formally, a hypergraph $\mathcal{G}^h = (\mathcal{V}, \mathcal{E}^h)$ consists of a set of nodes \mathcal{V} , and a set of non-empty subsets of \mathcal{V} , namely hyperedges \mathcal{E}^h . For each hyperedge $e \in \mathcal{E}^h$, we have $e = \{v_1, \dots, v_k\}$, $v_i \in \mathcal{V}$, $2 \leq k \leq |\mathcal{V}|$.

Line Graphs. Suppose $\mathcal{G} = (\mathcal{V}, \mathcal{E})$ is a finite undirected graph, we denote $L(\mathcal{G}) = (\mathcal{V}_L, \mathcal{E}_L)$ as the line graph of \mathcal{G} , i.e., the vertices of $L(\mathcal{G})$ are the edges of \mathcal{G} and two vertices of $L(\mathcal{G})$ are adjacent if their corresponding edges in \mathcal{G} have a node in common. The line graph of a directed graph \mathcal{G} only has one difference compared to the undirected version such that, an edge in $L(\mathcal{G})$ is built only when the two corresponding directed edges e_1 and e_2 satisfy that the head of e_1 is the tail of e_2 . Example constructions are shown in Fig. 2.

Incidence matrix $\mathbf{H} \in \mathbb{R}^{|\mathcal{V}| \times |\mathcal{V}_L|}$ builds the correspondence between $L(\mathcal{G})$ and \mathcal{G} with each entry $\mathbf{H}(v, v_L)$ determined by:

$$\mathbf{H}(v, v_L) = \begin{cases} 1, & \text{if } v \text{ belongs to } e \text{ (make } v_L) \\ 0, & \text{otherwise.} \end{cases} \quad (1)$$

We can construct a line graph out of a line graph in an iterated way. For simplicity, we express m -iterated line graph (m -ILG) $L(\dots(L(\mathcal{G})))$ as $L^m(\mathcal{G})$, and the incidence matrix is $\mathbf{H}^{(m)} = \mathbf{H}^{(0,1)} \dots \mathbf{H}^{(m-1,m)}$, where $\mathbf{H}^{(p,q)}$ links a p -ILG to a q -ILG.

Graph Convolutional Networks. Given a graph \mathcal{G} , the $(t+1)$ -th layer of GCN aggregate the neighborhood information of each node via

$$\mathbf{X}^{(t+1)} = \sigma\left(\tilde{\mathbf{A}}\mathbf{X}^{(t)}\mathbf{W}^{(t)}\right), \quad (2)$$

where \mathbf{X} is the node feature matrix, $\tilde{\mathbf{A}} = \tilde{\mathbf{D}}^{-\frac{1}{2}}(\mathbf{A} + \mathbf{I})\tilde{\mathbf{D}}^{-\frac{1}{2}}$ is the normalized adjacency matrix of \mathcal{G} with self-connections, $\tilde{\mathbf{D}}_{ii} = \sum_j (A_{ij} + 1)$ is a diagonal matrix, and $\sigma(\cdot)$ is an activation function.

Problem Definition

Let $\mathcal{G}_s = (\mathcal{V}_s, \mathcal{E}_s, \mathbf{X}_s, \mathbf{E}_s)$, $\mathcal{G}_t = (\mathcal{V}_t, \mathcal{E}_t, \mathbf{X}_t, \mathbf{E}_t)$ be the source and target graph respectively, which consist of a finite set of nodes $\mathcal{V} = \{v_1, \dots, v_{|\mathcal{V}|}\}$, a finite set of edges $\mathcal{E} = \{e_{ij}\}_{i,j=1}^{|\mathcal{V}|}$, an optional node feature matrix $\mathbf{X} \in \mathbb{R}^{|\mathcal{V}| \times \cdot}$ and an optional edge feature matrix $\mathbf{E} \in \mathbb{R}^{|\mathcal{E}| \times \cdot}$. W.l.o.g., we assume that $|\mathcal{V}_s| \leq |\mathcal{V}_t|$.

The problem of graph matching is as follows. Given \mathcal{G}_s and \mathcal{G}_t with adjacency matrices \mathbf{A}_s and \mathbf{A}_t respectively, we aim to find a mapping matrix $\mathbf{S} \in \{0, 1\}^{|\mathcal{V}_s| \times |\mathcal{V}_t|}$ which follows one-to-one mapping constraints $\sum_{j \in \mathcal{V}_t} S_{i,j} \leq 1, \forall i \in \mathcal{V}_s$ and $\sum_{i \in \mathcal{V}_s} S_{i,j} \leq 1, \forall j \in \mathcal{V}_t$. We infer an injective mapping function $\pi: \mathcal{V}_s \rightarrow \mathcal{V}_t$ which maps each node in \mathcal{G}_s to a node in \mathcal{G}_t . Conventionally, graph matching is expressed as an edge-preserving problem:

$$\mathbf{S} = \arg \min \left(\|\mathbf{A}_s - \mathbf{S}^T \mathbf{A}_t \mathbf{S}\|_F^2 \right), \quad (3)$$

subject to the one-to-one mapping constraints mentioned above. However, this formulation only leverages the local structure (edges) to find a mapping. In our work, we extend the local structural information to the high-order structural information by introducing iterated line graphs. One can interpret our problem as solving Eq. 3 with the adjacency matrices replaced with expressions concerning iterated line graphs for better alignment on the original graphs.

The Proposed Approach

Iterated Line Graph Construction

Given the source graph \mathcal{G}_s and the target graph \mathcal{G}_t , we construct the m -ILG $L^m(\mathcal{G}) = (\mathcal{V}^{(m)}, \mathcal{E}^{(m)}, \mathbf{A}^{(m)}, \mathbf{X}^{(m)})$ by the definition of ILGs. $\mathbf{A}^{(m)}$ and $\mathbf{X}^{(m)}$ are the adjacency matrix and the feature matrix of $L^m(\mathcal{G})$ respectively and can be constructed by setting k to $\{1, \dots, m\}$ iteratively in the following equations:

$$\begin{aligned} \mathbf{x}_i^{(k)} &= \bigoplus_j (\mathbf{H}^{(k-1,k)T})_{i,j} \mathbf{x}_j^{(k-1)}, \\ \mathbf{A}^{(k)} &= \mathbf{H}^{(k-1,k)T} \mathbf{H}^{(k-1,k)} - 2\mathbf{I}, \end{aligned} \quad (4)$$

where \bigoplus is the operation concatenating the non-zero vectors, and $\mathbf{X}^{(0)} = \mathbf{X}$ of the original graph.

Compared to the conventional hypergraph-based methods, we impose no additional information, e.g., community or cluster information, to construct ILGs. Hence our methods are more general in expressing hypergraph structure without additional attributes of the graph. More importantly, the high-order structural information, such as the relation across different hyperedges, is explicitly expressed with

ILGs, which is not captured in the previous definition of hypergraphs.

High-order Graph Matching

Given the m -ILGs of the source and the target graph, we implement Graph Neural Networks (GNNs) on $L^m(\mathcal{G}_s)$ and $L^m(\mathcal{G}_t)$ to learn the similarity between the two, which we referred to as m -order structural similarity. With the incidence matrices, we are able to project the m -order similarity to the similarity across the original source and target graph, expressed by \mathbf{S} :

$$\mathbf{S} = \text{sinkhorn}(\tilde{\mathbf{H}}_s^{(m)} \mathbf{Z}_s^{(m)} \mathbf{Z}_t^{(m)T} \tilde{\mathbf{H}}_t^{(m)T}), \quad (5)$$

where $\tilde{\mathbf{H}}^{(m)} = \mathbf{D}_{\mathbf{H}^{(m)}}^{-1} \mathbf{H}^{(m)}$, $\mathbf{D}_{\mathbf{H}^{(m)}} \in \mathbb{R}^{|\mathcal{V}| \times |\mathcal{V}|}$ is a diagonal matrix and $\mathbf{D}_{\mathbf{H}^{(m)}}(i, i) = \sum_j H_{i,j}^{(m)}$. $\mathbf{Z}_s^{(m)} = \Psi_{\theta_1}(\mathbf{X}_s^{(m)}, \mathbf{A}_s^{(m)}, \mathbf{E}_s^{(m)})$ and $\mathbf{Z}_t^{(m)} = \Psi_{\theta_1}(\mathbf{X}_t^{(m)}, \mathbf{A}_t^{(m)}, \mathbf{E}_t^{(m)})$ are ILG features computed from the shared GNN $\Psi_{\theta_1}(\cdot)$. Sinkhorn normalization is applied to obtain rectangular doubly-stochastic correspondence matrices that fulfill the one-to-one mapping constraints $\sum_{j \in \mathcal{V}_t} S_{i,j} = 1, \forall i \in \mathcal{V}_s$ and $\sum_{i \in \mathcal{V}_s} S_{i,j} \leq 1, \forall j \in \mathcal{V}_t$ (Sinkhorn and Knopp 1967). $\tilde{\mathbf{H}}^{(m)} \mathbf{Z}^{(m)}$ can be considered as features on the m -ILG projected to the original graph to match nodes in the original graphs.

In practice, we take the local structural information on the original graph into account, and calculate the similarity as a combination of the high-order and the local similarity:

$$\begin{aligned} \mathbf{S} = \text{sinkhorn} \left(\underbrace{\alpha (\tilde{\mathbf{H}}_s^{(m)} \mathbf{Z}_s^{(m)} \mathbf{Z}_t^{(m)T} \tilde{\mathbf{H}}_t^{(m)T})}_{\text{high-order similarity}} \right. \\ \left. + (1 - \alpha) \underbrace{(\mathbf{Z}_s \mathbf{Z}_t^T)}_{\text{local similarity}} \right), \end{aligned} \quad (6)$$

where $\mathbf{Z}_s = \Psi_{\theta_2}(\mathbf{X}_s, \mathbf{A}_s, \mathbf{E}_s)$, and $\mathbf{Z}_t = \Psi_{\theta_2}(\mathbf{X}_t, \mathbf{A}_t, \mathbf{E}_t)$. We train Ψ_{θ_1} and Ψ_{θ_2} by minimizing the cross entropy loss:

$$\mathcal{L} = - \sum_{i \in \mathcal{V}_s, j \in \mathcal{V}_t} S_{i,j}^{gt} \log(S_{i,j}) \quad (7)$$

where $S_{i,j}$ are the similarity to be learned and $S_{i,j}^{gt} = 1$ if and only if node $i \in \mathcal{G}_s$ has ground truth correspondence $j \in \mathcal{G}_t$.

We implement the siamese version of the GNN model, which has shown great advantage in capturing the similarity between different graphs (Li et al. 2019; Fey et al. 2020). Concretely, \mathcal{G}_s and \mathcal{G}_t share θ_2 of Ψ_{θ_2} for learning local similarity, $L^m(\mathcal{G}_s)$ and $L^m(\mathcal{G}_t)$ share θ_1 of Ψ_{θ_1} for learning high-order similarity. We implement Ψ_{θ_1} , Ψ_{θ_2} as the standard GNNs, which generally aggregate the structural information and update the node features $\mathbf{x}_v^{(t-1)}$ in layer t via

$$\begin{aligned} \mathbf{x}_{\mathcal{N}(v)}^{(t)} &= \text{AGGREGATE}^{(t)}(\mathbf{x}_u^{(t-1)}, \forall u \in \mathcal{N}(v)), \\ \mathbf{x}_v^{(t)} &= \text{UPDATE}^{(t)}(\mathbf{x}_v^{(t-1)}, \mathbf{x}_{\mathcal{N}(v)}^{(t)}), \end{aligned} \quad (8)$$

where $\mathcal{N}(v)$ is the neighbor set of node v on the original or any order of the ILGs. Fig. 3 shows our HGMM frameworks based on ILGs.

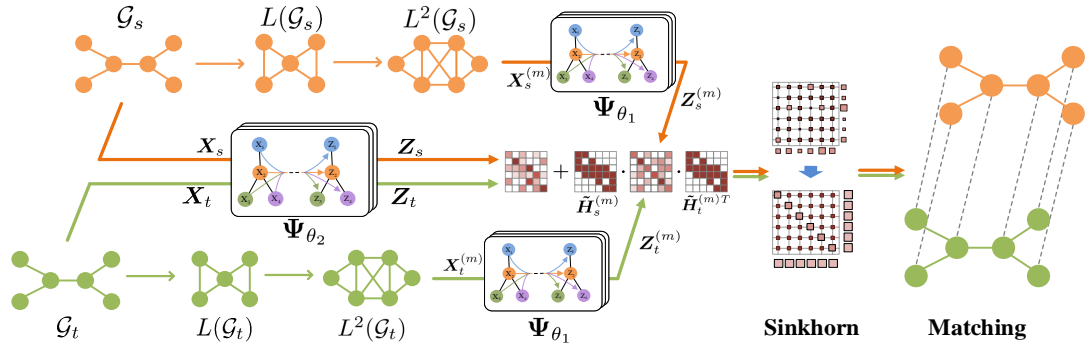


Figure 3: Overview of our high-order graph matching networks with iterated line graphs. Features of iterated line graphs and original graphs are learned by GNNs. Inner product is used to calculate the distance between node pairs and the weighted sum of the local and high-order corresponding matrices. Sinkhorn operations produce the one-to-one matching results.

We will show how the ILG is related to the GCNs model with the Thm. 1, and further display the unique advantage of our method in Thm. 2.

Theorem 1. *The feature on the line graph is equivalently expressive as that of the one-layer GCN.*

The proof of Thm. 1 can be found in the supplementary materials. We further found that ILGs are capable of describing high-order structural information which are missed by GCNs. Before introducing the Thm. 2, we show the following lemma holds true:

Lemma 1. *Let \mathbf{A} be the adjacency matrix of graph \mathcal{G} , \mathbf{A}^m is \mathbf{A} raised to the m -th power, and $\mathbf{H}^{(m)}$ be the incidence matrix of m -ILG $L^m(\mathcal{G})$. We have $\mathbf{1}_{[(\mathbf{A}+\mathbf{I})^m > 0]} = \mathbf{1}_{[\mathbf{H}^{(m)}\mathbf{H}^{(m)T} > 0]}$ where $\mathbf{1}_{[x > 0]}$ represents that the element x is set to 1 where $x > 0$ in \mathbf{X} .*

With Lemma 1, we can prove the following theorem:

Theorem 2. *ILGs are strictly more expressive than GCNs in expressing high-order structural information.*

We have proven that m -layer GCNs without non-linear layers only capture the nodes within m -hop neighborhood of node $i \in \mathcal{G}$, without considering the relative positions of the nodes. While in m -ILG, the relations between different hyperedges are explicitly expressed and learned. Hence we think the ILG captures richer high-order structural information than GCNs.

Hierarchical Variants

Since Eq. 6 only considers the m -th order similarity between $L^m(\mathcal{G}_s)$ and $L^m(\mathcal{G}_t)$, as well as the local similarity between \mathcal{G}_s and \mathcal{G}_t , some crucial structural similarity information between $L^k(\mathcal{G}_s)$ and $L^k(\mathcal{G}_t)$ ($1 \leq k < m$), may be missed. Hence we propose a hierarchical variant of HGMM by training similarity \mathbf{S} on the k -ILG from $k = 0$ to $k = m$ independently and iteratively. After the training on the $(k - 1)$ -ILG is done, we initialize the feature of the k -ILG (source and target) as

$$\mathbf{x}_i^{(k)} = \bigoplus_j ((\mathbf{H}^{(k-1,k)})^T)_{i,j} (\mathbf{Z}^{(k-1)})_j, \quad (9)$$

where $\mathbf{Z}^{(k-1)}$ is learned on the $(k - 1)$ -ILG. In the hierarchical variant, k -th order features are built iteratively. We do not train features of order 0 to m in an end-to-end fashion due to the high complexity issue.

Complexity Analysis

The time complexity of HGMM is determined by the complexity of GNN used. The space complexity is decided by sizes of ILGs. Assuming $d_{max}^{(m)}$ is the max degree of m -ILG $L^m(\mathcal{G})$, the upper bound of the size of $L^m(\mathcal{G})$ can be expressed as $|\mathcal{V}| \prod_{l=0}^m (d_{max}^{(l)}/2)$, given \mathcal{G} with $|\mathcal{V}|$ nodes. To see it, we first obtain the upper bound of the number of edges of \mathcal{G} as $|\mathcal{V}|(d_{max}^{(0)}/2)$, which is also the upper bound of $|\mathcal{V}^{(1)}|$ in $L(\mathcal{G})$. The upper bound of $|\mathcal{V}^{(m)}|$ can be obtained iteratively.

To calculate the corresponding matrix \mathbf{S} in Eq. 6, it is required to store $\tilde{\mathbf{H}}^{(m)} \in \mathbb{R}^{|\mathcal{V}| \times |\mathcal{V}^{(m)}|}$, $\mathbf{Z}^{(m)} \in \mathbb{R}^{|\mathcal{V}^{(m)}| \times k}$, $\tilde{\mathbf{H}}^{(m)} \mathbf{Z}^{(m)} \in \mathbb{R}^{|\mathcal{V}| \times k}$, for both the source and target graph, where k is the feature dimension of node in $L^m(\mathcal{G})$. Hence the space complexity of Eq. 6 is $O(\sum_{i \in \{s,t\}} (|\mathcal{V}_i|^2 \prod_{l=0}^m (d_{max}^{(l)}/2) + k |\mathcal{V}_i| \prod_{l=0}^m (d_{max}^{(l)}/2) + k |\mathcal{V}_i|) + |\mathcal{V}_s| |\mathcal{V}_t|)$. Since the k -th order hierarchical variant is learned over the $(k - 1)$ -ILG, the space complexity depends on the highest order m . Such complexity is much smaller than that of high-order affinity tensor based method (Duchenne et al. 2011), which is $O((|\mathcal{V}_s| |\mathcal{V}_t|)^m)$, on large graphs.

Scaling To Large Graphs

Although the complexity of HGMM is low compared to other schemes, it is still unacceptable for large-scale graphs. Hence we apply several optimization techniques to make HGMM more scalable in practice.

Edge deletion. According to the above complexity analysis, d_{max} is an important factor to the space complexity. Hence we can control the complexity with a preset hyperparameter $d^{(k)}$ to constrain the size of the k -ILG. Specifically, to construct $L^{k+1}(\mathcal{G})$, we randomly select $\min\{|\mathcal{N}(v^{(k)})|, d^{(k)}\}$ neighbors of $v^{(k)}$ in $L^k(\mathcal{G})$ to keep the edges of $v^{(k)}$ connected to these neighbors and delete others. Note that we do not delete anything related to the nodes with ground truth as the information is crucial in training.

Sparse correspondences. Following the work of (Fey et al. 2020), we also sparsify correspondence matrix \mathbf{S} by filtering out the low rank correspondences. Concretely, we compute Top_k correspondences of each row $\mathbf{S}_{i,:}$, and store its sparse version including the ground truth entries $\mathbf{S}_{i,\pi(i)}$.

Table 1: Real-world dataset used in our experiments, where d_{max} is the max degree of each network.

Dataset		$ \mathcal{V} $	$ \mathcal{E} $	d_{max}	Seeds
Twitter	\mathcal{G}_s	5220	164919	1725	1609
Foursquare	\mathcal{G}_t	5315	76972	552	
AI	\mathcal{G}_s	12029	67760	116	1136
DM	\mathcal{G}_t	8916	55112	145	
AI _{13,14}	\mathcal{G}_s	7226	25081	73	2861
AI _{15,16}	\mathcal{G}_t	10241	43534	73	
DBP _{FR}	\mathcal{G}_s	19661	105998	145	15000
DBP _{EN}	\mathcal{G}_t	19993	115722	142	
DBP _{JA}	\mathcal{G}_s	19814	77214	76	15000
DBP _{EN}	\mathcal{G}_t	19780	93484	135	
DBP _{ZH}	\mathcal{G}_s	19388	70414	73	15000
DBP _{EN}	\mathcal{G}_t	19572	95142	90	

Although it still requires $O(|\mathcal{V}_s||\mathcal{V}_t|)$ to store the dense version of \mathcal{S} , the space consumption in the backpropagation stage is reduced by a large margin.

Experiments

We verify our approach in three different settings. To avoid the cascaded expansion of high-order line graphs, we limit the highest order m to 2. k -HGMM ($k \in \{0, 1, 2\}$) means HGMM is performed on the k -iterated line graph. In particular, 0-HGMM only utilizes information on original graph and thus can be considered as a variant of GNNs. In addition, 0-1-HGMM and 0-1-2-HGMM are the hierarchical variants with $m=1$ and $m=2$ respectively. We first demonstrate our method in an ablation study on synthetic graphs, and apply it to real-world tasks in social networks and cross-lingual knowledge graph alignment afterwards.

Datasets and Metrics

Our datasets include: **1) Twitter-Foursquare.** The two social networks are collected from Foursquare and Twitter (Zhang and Philip 2015). **2) AI-DM.** Two co-author networks are extracted from papers published between 2014 and 2016 (collected by Acemap) in 8 representative conferences on Artificial Intelligence (AI) and Data Mining (DM) ¹ respectively. **3) AI_{13,14}-AI_{15,16}.** Two co-author networks are constructed on papers published in 8 AI conferences (collected by Acemap) in 2013-2014 and 2015-2016 respectively. **4) DBP15K.** The datasets are generated from the multilingual versions of DBpedia (Sun, Hu, and Li 2017), which pair entities of the knowledge graphs in French, Japanese and Chinese into the English version and vice versa. All dataset statistics are listed in Table 1.

Following most works (Zhou et al. 2018; Fey et al. 2020), we adopt the standard metric $Precision@k(P@k)$ to evaluate the matching performance, which measures the proportion of correctly matched pairs ranked in the top k .

Ablation Study on Synthetic Graphs

We evaluate HGMM on synthetic graphs. We first construct an undirected Erdos-Renyi graph as the source graph \mathcal{G}_s with $|\mathcal{V}_s| = 100$ nodes and edge probability $p = 0.1$,

¹AI conferences are IJCAI, AAAI, CVPR, ICCV, ICML, NeurIPS, ACL, and EMNLP, whereas the DM conferences include KDD, SIGMOD, SIGIR, ICDM, ICDE, VLDB, WWW, and CIKM.

and a target graph \mathcal{G}_t which is built from \mathcal{G}_s by randomly deleting edges with probability p_d . For each $p_d \in \{0.0, 0.1, 0.2, 0.3, 0.4, 0.5\}$, 100 pairs of source and target graphs are generated and trained to report the average results.

Architecture and parameters. We implement Ψ_{θ_1} and Ψ_{θ_2} by stacking T layers of Graph Isomorphism Network (GIN) operator (Xu et al. 2019a):

$$\mathbf{x}_i^{(t)} = \text{MLP}^{(t)}\left(\left(1 + \epsilon^{(t)}\right) \cdot \mathbf{x}_i^{(t-1)} + \sum_{j \in \mathcal{N}(i)} \mathbf{x}_j^{(t-1)}\right), \quad (10)$$

considering its great power in distinguishing graph structures. Each MLP has a total number of layers 2 and hidden dimensionality of 100. The embedding for each node in \mathcal{G}_s and \mathcal{G}_t is initialized with one-hot encodings of node degrees. Following the setting of (Fey et al. 2020), we apply ReLU activation and Batch normalization after each layer, and utilize *Jumping Knowledge Style Concatenation* $\mathbf{x}_i = \mathbf{W}[\mathbf{x}_i^{(1)}, \dots, \mathbf{x}_i^{(T)}]$ to acquire the final node representation. We set $\alpha = 0.9$ in Eq. 6 and training ratio $T_r = 0.7$ by default without specific mentioning.

Results. Fig. 4(a) shows the matching accuracy P@1 for different structural noise p_d with $T = 3$. Benefiting from leveraging high-order and hierarchical structural information, 0-1-HGMM and 0-1-2-HGMM consistently outperform 0-HGMM. However, we observe that 1-HGMM and 2-HGMM are not always better than 0-HGMM. The difference is mostly caused by the initialization methods, as k -HGMM encodes the initial node features in k -ILG as combinations of the one-hot embeddings of corresponding nodes in the original graph, which is inferior than using the feature embeddings of $(k - 1)$ -HGMM. More specifically, 0-1-2-HGMM has better performance than 0-1-HGMM, but the improvement is much smaller than that from 0-HGMM to 0-1-HGMM. This reflects that the marginal benefit of learning high-order structural information is getting small with the increase of the order. Hence, a constant k may exist that $(k - 1)$ -HGMM is superior to k -HGMM.

Fig. 4(b) visualizes the P@1 accuracy for different numbers of layers. It can be observed that the performance of 0-HGMM drops when $T > 9$, due to the overfitting and over-smoothing problem, which is in accords with the conclusion in (Rong et al. 2019). Conversely, the hierarchical variants acquire more stable P@1 scores as ILG incorporates high-order information such that deeper GIN obtains better performance.

Fig. 4(c) and 4(d) show the P@1 accuracies for different values of hyperparameters. We set $T = 3$ and $p_d = 0.3$ in Fig. 4(c), $T = 16$ and $p_d = 0.3$ in Fig. 4(d). Fig 4(c) demonstrates that as the high-order information plays a growingly important part with the increase of α , the accuracies increase except for $\alpha = 0.9$. Fig. 4(d) shows the performance of HGMM on the Top_k correspondences. We observe that by choosing appropriate k s, the performance on the sparse correspondences is as good as that of the dense ones indicated by solid lines.

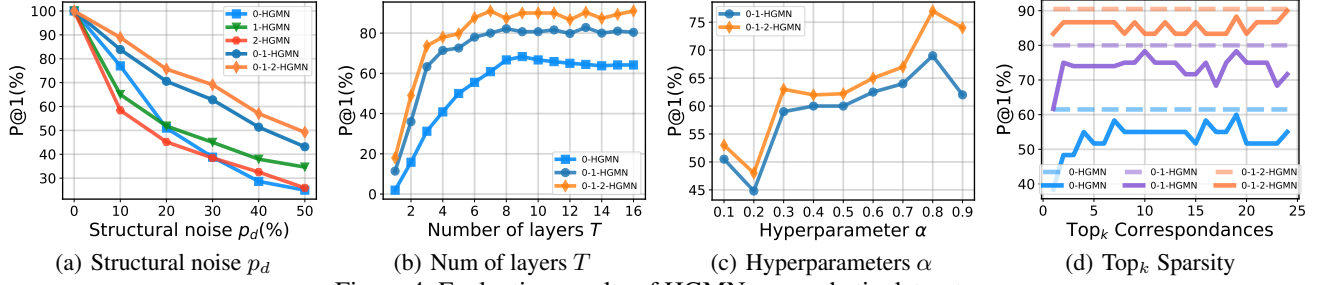


Figure 4: Evaluation results of HGMN on synthetic datasets.

Table 2: The $P@k(\%)$ results for the training ratio $Tr = 30\%$. Matching accuracies exceeding all baselines are marked in bold. The highest accuracies are underscored.

Method	Twitter-Foursquare			AI-DM			AI _{13,14} -AI _{15,16}		
	@1	@10	@30	@1	@10	@30	@1	@10	@30
IONE(Liu et al. 2016)	3.3	18.6	31.4	5.7	26.4	36.6	7.5	30.1	43.2
DeepLink(Zhou et al. 2018)	2.1	11.5	23.0	1.8	16.6	28.9	2.7	23.6	35.1
CrossMNA(Chu et al. 2019)	4.1	16.4	27.2	6.5	28.1	35.8	6.4	30.2	42.4
MGCN(Chen et al. 2020)	1.2	7.0	12.9	1.5	15.5	21.7	1.9	15.6	26.1
DGMC(Fey et al. 2020)	1.5	15.7	30.2	2.9	29.0	40.6	2.2	26.7	41.4
CGRW	1.2	11.8	23.3	2.5	26.9	41.6	0.4	22.5	39.2
GCN	5.5	25.3	40.6	4.3	32.4	46.0	5.9	36.2	51.5
1-HGMN	8.2	29.6	44.4	6.4	32.5	46.8	9.3	37.2	51.9
2-HGMN	9.2	31.9	47.0	6.1	32.7	47.1	9.9	37.2	51.8
0-1-HGMN	8.8	31.7	46.4	5.5	32.5	47.4	10.2	37.5	52.1
0-1-2-HGMN	10.1	32.3	48.3	6.7	32.7	48.9	10.4	36.2	51.5

Social Network Matching

We evaluate HGMN on three real-world social networks: Twitter-Foursquare, AI-DM and AI_{13,14}-AI_{15,16}. All graphs are anonymous and only structural information can be used. Since HGMN is not embedding-based, we initialize each feature by *Cross Graph Random Walk* (CGRW), which builds cross-network edges according to the ground truth and applies DeepWalk (Perozzi, Al-Rfou, and Skiena 2014) method.

Architecture and parameters. GCN (Kipf and Welling 2016) is adopted as our GNN operator:

$$\mathbf{X}^{(t+1)} = \sigma\left(\tilde{\mathbf{D}}^{-\frac{1}{2}} \tilde{\mathbf{A}} \tilde{\mathbf{D}}^{-\frac{1}{2}} \mathbf{X}^{(t)} \mathbf{W}^{(t)}\right). \quad (11)$$

Following each GCN layer, two MLP layers with 100 hidden units are attached. We set $\alpha = 0.5$, $T = 3$ and the training ratio $Tr = 0.3$. Moreover, the techniques of edge deletion and sparse correspondences are adopted. Hyperparameters include: $m = 2$, $d^{(0)} = 10$, $d^{(1)} = 5$, and $\text{Top}_k = 10$.

Results. We report P@1, P@10 and P@30 accuracies of all methods in Table 2. HGMN achieves the highest P@k among all methods under different k s. In particular, HGMN outperforms those GCN-based methods, *i.e.*, DGMC and GCN (0-HGMN) with three-layer GCNs, which shows the effectiveness of our method and highlights the benefits of introducing high-order structural information. Although we use CGRW as the initialization method, it does not contribute to the high accuracy as the performance of CGRW is far inferior to HGMN.

Across different variants of HGMN, 0-1-2-HGMN is more advantageous on Twitter-Foursquare and AI-DM dataset than on AI_{13,14}-AI_{15,16}. One possible reason is that the former two datasets have more complicated structures and heterogeneous attributes than the third one. When two corresponding nodes have more discrepant neighbors, more sophisticated methods are required to extract the local structures. Otherwise, the higher-order information would result in overfitting on graphs of homogeneous local structures. We also complement a series of experiments to identify the influence of Sinkhorn since some baselines are originally performed without Sinkhorn. The results are in the supplementary material.

Cross-Lingual Knowledge Graph Alignment

We also evaluate HGMN on the DBP15K dataset with directed and attributed graphs. We follow the setup of (Fey et al. 2020) by using the sum of word embeddings acquired by monolingual *FASTTEXT* embeddings as the final entity input representation.

Architecture and parameters. By referring to (Fey et al. 2020), we implement GNN operator Ψ_{θ_1} and Ψ_{θ_2} as

$$\mathbf{x}_i^{(t+1)} = \sigma\left(\mathbf{W}_1^{(t+1)} \mathbf{x}_i^{(t)} + \sum_{j \in \mathcal{N}_{in}(i)} \mathbf{W}_2^{(t+1)} \mathbf{x}_j^{(t)} + \sum_{j \in \mathcal{N}_{out}(i)} \mathbf{W}_3^{(t+1)} \mathbf{x}_j^{(t)}\right) \quad (12)$$

Table 3: The $P@k(\%)$ results for DBP15K dataset. Matching accuracies exceeding all baselines are marked in bold. The highest accuracies are underscored.

Method	ZH→EN		EN→ZH		JA→EN		EN→JA		FR→EN		EN→FR	
	@1	@10	@1	@10	@1	@10	@1	@10	@1	@10	@1	@10
GCN (Wang et al. 2018)	41.25	74.38	36.49	69.94	39.91	74.46	38.42	71.81	37.29	74.49	36.77	73.06
BOOTE (Sun et al. 2018)	62.94	84.75	60.98	81.29	62.26	85.39	58.25	83.10	65.30	87.44	61.79	85.08
MUGNN (Cao et al. 2019)	49.40	84.40	48.12	83.34	50.10	85.70	48.56	84.98	49.60	87.00	49.05	86.66
NAEA (Zhu et al. 2019)	65.01	86.73			64.41	87.27			67.32	89.43		
RDGCN (Wu et al. 2019)	70.75	84.55	67.73	84.53	76.74	89.54	74.53	89.24	88.64	95.72	86.80	95.41
GMNN (Xu et al. 2019b)	67.93	78.48	65.28	79.64	73.97	87.15	71.29	84.63	89.38	95.25	88.18	94.75
DGMC (Fey et al. 2020)	80.12	87.49	76.77	83.56	84.80	89.74	81.09	86.84	93.34	96.03	91.95	95.28
0-HGMN	78.89	91.84	73.92	88.67	81.01	93.44	80.74	93.12	91.85	97.74	90.61	97.51
1-HGMN	81.56	93.46	78.09	91.13	85.05	95.57	82.75	94.82	93.20	98.46	92.49	98.13
2-HGMN	80.74	93.64	76.93	90.85	84.17	95.46	82.08	94.19	92.10	98.43	91.52	98.07
0-1-HGMN	79.07	92.34	75.30	89.70	81.77	94.29	79.15	92.84	91.62	97.96	90.15	97.77
0-1-2-HGMN	73.49	90.13	71.57	84.77	77.27	92.38	74.89	91.31	87.22	96.88	87.53	96.70

where σ is the ReLU activation function. We set $T = 3$, $\alpha = 0.5$, and $\text{Top}_k = 10$. And edge deletion are adopted with $d^{(0)} = 5$ and $d^{(1)} = 1$.

Results. As shown in Table 3, HGMN outperforms the state-of-the-art (including 0-HGMN) on all pairs of graphs with accuracy gain up to 7.95%. Our method is still superior to the GCN-based methods GCN and GMNN, while GCN and GMNN both adopt two-layer GCNs. Benefitting from reaching a data-driven neighborhood consensus between matched node pairs, DGMC surpasses GMNN and 0-HGMN in $P@1$. The hierarchical variants of HGMN are in general inferior to k -HGMN, and this may be because the source and target graphs of DBP15K share homogeneous local structures. The table also shows that 1-HGMN has better performance than 2-HGMN. This is consistent with the discussion in the ablation study where the higher-order ILG may not always bring better performance. Overall, the high-order structural information of directed graphs can be captured by ILGs and brings significant improvement.

Conclusion

To utilize high-order information on graphs, we propose a novel method called HGMN for graph matching. By introducing the iterated line graph in our framework, we leverage high-order information in a principled way and prove that our method is more expressive than GCNs in aligning corresponding nodes across graphs. Hierarchical variants of HGMN are also proposed to exploit the hierarchical representation of graphs. Evaluated on a variety of real-world datasets, HGMN has shown superior matching performance than the state-of-the-art.

References

Cao, Y.; Liu, Z.; Li, C.; Li, J.; and Chua, T.-S. 2019. Multi-channel graph neural network for entity alignment. *ACL*.

Chen, H.; Yin, H.; Sun, X.; Chen, T.; Gabrys, B.; and Musial, K. 2020. Multi-level Graph Convolutional Networks for Cross-platform Anchor Link Prediction. *Proceedings of*

the 26th ACM SIGKDD International Conference on Knowledge Discovery and Data Mining 1503–1511.

Cho, M.; Lee, J.; and Lee, K. M. 2010. Reweighted random walks for graph matching. In *European conference on Computer vision*, 492–505. Springer.

Chu, X.; Fan, X.; Yao, D.; Zhu, Z.; Huang, J.; and Bi, J. 2019. Cross-network embedding for multi-network alignment. In *The World Wide Web Conference*, 273–284.

Duchenne, O.; Bach, F.; Kweon, I.-S.; and Ponce, J. 2011. A tensor-based algorithm for high-order graph matching. *IEEE transactions on pattern analysis and machine intelligence* 33(12): 2383–2395.

Fey, M.; Lenssen, J. E.; Morris, C.; Masci, J.; and Kriege, N. M. 2020. Deep Graph Matching Consensus. In *International Conference on Learning Representations*.

Fu, L.; Zhang, J.; Wang, S.; Wu, X.; Wang, X.; and Chen, G. 2020. De-Anonymizing Social Networks With Overlapping Community Structure. *IEEE/ACM Transactions on Networking* 28(1): 360–375.

Harary, F.; and Norman, R. Z. 1960. Some properties of line digraphs. *Rendiconti del Circolo Matematico di Palermo* 9(2): 161–168.

Kipf, T. N.; and Welling, M. 2016. Semi-supervised classification with graph convolutional networks. *International Conference on Learning Representations*.

Li, Y.; Gu, C.; Dullien, T.; Vinyals, O.; and Kohli, P. 2019. Graph Matching Networks for Learning the Similarity of Graph Structured Objects. *Proceedings of the 36th international conference on machine learning (ICML-19)*.

Liu, L.; Cheung, W. K.; Li, X.; and Liao, L. 2016. Aligning Users across Social Networks Using Network Embedding. In *IJCAI*, 1774–1780.

Loiola, E. M.; de Abreu, N. M. M.; Boaventura-Netto, P. O.; Hahn, P.; and Querido, T. 2007. A survey for the quadratic assignment problem. *European journal of operational research* 176(2): 657–690.

- Morris, C.; Ritzert, M.; Fey, M.; Hamilton, W. L.; Lenssen, J. E.; Rattan, G.; and Grohe, M. 2019. Weisfeiler and leman go neural: Higher-order graph neural networks. In *Proceedings of the AAAI Conference on Artificial Intelligence*, volume 33, 4602–4609.
- Nguyen, Q.; Gautier, A.; and Hein, M. 2015. A flexible tensor block coordinate ascent scheme for hypergraph matching. In *Proceedings of the IEEE Conference on Computer Vision and Pattern Recognition*, 5270–5278.
- Perozzi, B.; Al-Rfou, R.; and Skiena, S. 2014. Deepwalk: Online learning of social representations. In *Proceedings of the 20th ACM SIGKDD international conference on Knowledge discovery and data mining*, 701–710. ACM.
- Rong, Y.; Huang, W.; Xu, T.; and Huang, J. 2019. Droppedge: Towards deep graph convolutional networks on node classification. In *International Conference on Learning Representations*.
- Sinkhorn, R.; and Knopp, P. 1967. Concerning nonnegative matrices and doubly stochastic matrices. *Pacific Journal of Mathematics* 21(2): 343–348.
- Sun, Z.; Hu, W.; and Li, C. 2017. Cross-lingual entity alignment via joint attribute-preserving embedding. In *International Semantic Web Conference*, 628–644. Springer.
- Sun, Z.; Hu, W.; Zhang, Q.; and Qu, Y. 2018. Bootstrapping Entity Alignment with Knowledge Graph Embedding. In *IJCAI*, 4396–4402.
- Tan, S.; Guan, Z.; Cai, D.; Qin, X.; Bu, J.; and Chen, C. 2014. Mapping users across networks by manifold alignment on hypergraph. In *Twenty-Eighth AAAI Conference on Artificial Intelligence*.
- Wang, R.; Yan, J.; and Yang, X. 2019. Learning combinatorial embedding networks for deep graph matching. In *Proceedings of the IEEE International Conference on Computer Vision*, 3056–3065.
- Wang, Z.; Lv, Q.; Lan, X.; and Zhang, Y. 2018. Cross-lingual knowledge graph alignment via graph convolutional networks. In *Proceedings of the 2018 Conference on Empirical Methods in Natural Language Processing*, 349–357.
- Wu, Y.; Liu, X.; Feng, Y.; Wang, Z.; Yan, R.; and Zhao, D. 2019. Relation-aware entity alignment for heterogeneous knowledge graphs. *Proceedings of the Twenty-Eighth International Joint Conference on Artificial Intelligence (IJCAI-19)*.
- Xu, K.; Hu, W.; Leskovec, J.; and Jegelka, S. 2019a. How powerful are graph neural networks? *International Conference on Learning Representations*.
- Xu, K.; Wang, L.; Yu, M.; Feng, Y.; Song, Y.; Wang, Z.; and Yu, D. 2019b. Cross-lingual knowledge graph alignment via graph matching neural network. *ACL*.
- Yan, J.; Zhang, C.; Zha, H.; Liu, W.; Yang, X.; and Chu, S. M. 2015. Discrete hyper-graph matching. In *Proceedings of the IEEE conference on computer vision and pattern recognition*, 1520–1528.
- Zass, R.; and Shashua, A. 2008. Probabilistic graph and hypergraph matching. In *2008 IEEE Conference on Computer Vision and Pattern Recognition*, 1–8. IEEE.
- Zhang, J.; and Philip, S. Y. 2015. Integrated anchor and social link predictions across social networks. In *Twenty-Fourth International Joint Conference on Artificial Intelligence*.
- Zhou, F.; and De la Torre, F. 2015. Factorized graph matching. *IEEE transactions on pattern analysis and machine intelligence* 38(9): 1774–1789.
- Zhou, F.; Liu, L.; Zhang, K.; Trajcevski, G.; Wu, J.; and Zhong, T. 2018. Deeplink: A deep learning approach for user identity linkage. In *IEEE INFOCOM 2018-IEEE Conference on Computer Communications*, 1313–1321. IEEE.
- Zhu, Q.; Zhou, X.; Wu, J.; Tan, J.; and Guo, L. 2019. Neighborhood-Aware Attentional Representation for Multilingual Knowledge Graphs. In *Twenty-Eighth International Joint Conference on Artificial Intelligence IJCAI-19*.